

Nano granular metallic Fe - oxygen deficient $\text{TiO}_{2-\delta}$ composite films: A room temperature, highly carrier polarized magnetic semiconductor

S. D. Yoon,* C. Vittoria,[†] and V. G. Harris[‡]
*Center for Microwave Magnetic Materials and Integrated Circuits,
Department of Electrical and Computer Engineering,
Northeastern University, Boston, MA. 02115 USA*

A. Widom[§]
Department of Physics, Northeastern University, Boston, MA. 02115 USA.

K. E. Miller and M. E. McHenry
*Department of Material Science and Engineering,
Carnegie Mellon University, Pittsburgh, PA. 15213, USA.*

Nano granular metallic iron (Fe) and titanium dioxide ($\text{TiO}_{2-\delta}$) were co-deposited on (100) lanthanum aluminate (LaAlO_3) substrates in a low oxygen chamber pressure using a pulsed laser ablation deposition (PLD) technique. The co-deposition of Fe and TiO_2 resulted in ≈ 10 nm metallic Fe spherical grains suspended within a $\text{TiO}_{2-\delta}$ matrix. The films show ferromagnetic behavior with a saturation magnetization of 3100 Gauss at room temperature. Our estimate of the saturation magnetization based on the size and distribution of the Fe spheres agreed well with the measured value. The film composite structure was characterized as p-type magnetic semiconductor at 300 K with a carrier density of the order of $10^{22}/\text{cm}^3$. The hole carriers were excited at the interface between the nano granular Fe and $\text{TiO}_{2-\delta}$ matrix similar to holes excited in the metal/n-type semiconductor interface commonly observed in Metal-Oxide-Semiconductor (MOS) devices. From the large anomalous Hall effect directly observed in these films it follows that the holes at the interface were strongly spin polarized. Structure and magneto transport properties suggested that these PLD films have potential nano spintronics applications.

PACS numbers: 75.50.Pp, 71.30.+h, 72.20.-i, 71.70.Gm, 72.25.-b, 73.40.Qv

I. INTRODUCTION

The search for semiconductors exhibiting magnetism at room temperature has been long and unyielding. However, recently much progress has been made toward this goal^{1,2,3,4,5,6,7}. By doping a host semiconductor material with transition metal ferromagnetic atoms, dilute ferromagnetic semiconductors have been produced with Curie temperatures (T_c) as high as 100 K¹. Hall effect measurements below T_c showed evidence for carriers being spin polarized raising hopes for spintronics applications. Specifically, metallic manganese (Mn) was doped into gallium arsenide (GaAs) whereby the carriers were strongly spin polarized¹.

We have previously reported the magnetic and de-transport properties of magnetic semiconductor films of $\text{TiO}_{2-\delta}$, where δ indicates the degree of oxygen deficiency or defects in the film^{8,9,10}. The Curie temperature, $T_c \approx 880$ K, was well above room temperature with a saturation magnetization, $4\pi M_S \approx 400$ Gauss. Titanium dioxide, TiO_2 , is a well known wideband gap oxide semiconductor, belonging to the group IV-VI semiconductors, described in terms of an ionic model of Ti^{4+} and O^{2-} ^{11,12,13,14,15}. Its intriguing dielectric properties allow its use as a gate insulator material in the Field-Effect-Transistor (FET)¹⁶. Also, TiO_2 is characterized to be an n-type semiconductor with an energy gap varying in the range $3 \text{ volt} < \frac{\Delta}{e} < 9 \text{ volt}$ depending on

sample preparation^{11,12,13,14,15}. Films of $\text{TiO}_{2-\delta}$ on substrates of (100) lanthanum aluminate (i.e. LaAlO_3) were deposited by a pulsed laser ablation deposition (PLD) technique at various oxygen chamber pressures ranging from 0.3 to 400 mtorr. The origin of the presence of Ti^{2+} and Ti^{3+} (as well as Ti^{4+}) ions was postulated as a result of the low oxygen chamber pressure during the films growth⁹. Oxygen defects gave rise to valence states of Ti^{2+} and Ti^{3+} (in the background of Ti^{4+}) whereby double exchange between these sites dominated. The same carriers involved in double exchange also gave rise to impurity donor levels accounting for the transport properties of the film. The dilute number of carriers were polarized in external applied magnetic field, yet the magnetic moment was still rather small¹⁰. For example, normal Hall resistivity was measured to be much bigger than the anomalous Hall resistivity¹⁰. In order to increase the anomalous contribution to the Hall effect and thereby increase the number of polarized carriers, we have fabricated a nano-granular (NG) metallic iron (Fe) in semiconducting $\text{TiO}_{2-\delta}$ matrix. The intent was to introduce a substantial magnetization component internally to the semiconductor $\text{TiO}_{2-\delta}$.

The basic difference between our film composite and the previously reported magnetic semiconductors by others is that in our films the NG of metallic Fe co-exist in a metallic state, whereas magnetic semiconductors prepared by others the transition metal co-exists as metal

oxides and often oxide clusters^{4,5,6,7}. This major difference is important in terms of the magnetic and transport properties of the magnetic semiconductor presently produced by us and that of others^{4,5,6,7}. For example, NG metallic Fe contains a significant higher moment and Curie temperature than any other transition metal oxides. Also, the presence of NG metallic Fe allows for the creation of a reservoir of conduction electrons in the conduction band and, therefore, holes in the $\text{TiO}_{2-\delta}$ matrix. As electrons from the conduction band of $\text{TiO}_{2-\delta}$ are thermally introduced into the metallic Fe conduction band, holes are created in $\text{TiO}_{2-\delta}$ much like in junctions of NG metal/semiconductor interfaces or in Metal Oxide Semiconductor (MOS) devices¹⁷. Conduction of holes occurs in the $\text{TiO}_{2-\delta}$ host. This mechanism gives rise to lower resistivity at high temperature in contrast to the pure $\text{TiO}_{2-\delta}$ reported earlier^{9,10} where the carriers were only electrons. No such mechanism is possible in magnetic semiconductors doped with transition metal oxides. We report here that in our composite films of NG metallic Fe in anatase $\text{TiO}_{2-\delta}$ the magnetization, $4\pi M_S \approx 3,100$ Gauss (also $\approx 0.4\mu_B/\text{Fe}$), at room temperature, T_c above 800 K, the carriers are strongly spin polarized and the room temperature resistivity is lowered by a factor of $\approx 10^{-3}$ relative to films of the undoped $\text{TiO}_{2-\delta}$ semiconductors previously produced^{8,9,10}. Experimental results, discussions and concluding remarks follow.

II. EXPERIMENTAL RESULTS AND ANALYSIS

Thin films consisting of nano granular (NG) metallic Fe and $\text{TiO}_{2-\delta}$ were deposited by a pulsed laser ablation deposition (PLD) technique from binary targets of TiO_2 and metallic Fe on (100) LaAlO_3 substrates. Targets of TiO_2 and Fe were mounted on a target rotator driven by a servomotor and synchronized with the trigger of the pulsed excimer laser $\lambda = 248$ nm. In each deposition cycle, the ratio of laser pulses incident upon the TiO_2 target to those upon the Fe target was 6:1, this technique denoted as alternating targets-pulsed laser ablation deposition (AT-PLD) technique. The substrate temperature, laser energy density, and pulse repetition rate were maintained at 700 °C, ≈ 8.9 J/cm², and 1 Hz, respectively. The deposition was carried out in a pure oxygen background of around 10^{-5} torr in order to induce defects in the TiO_2 host. There were a total of 4,206 laser pulses (3,606 pulses on TiO_2 target and 600 pulses on Fe target) for each film resulting in a thickness of approximately 200 nm as measured by a Dek-Tek step profilometer.

Crystallographic and micrographic properties of the AT-PLD films were measured using x-ray diffractometry (XRD) and transmission electron microscopy (TEM). Results indicate phases of anatase TiO_2 , metallic body centered cubic (bcc) Fe. (001) plane of anatase $\text{TiO}_{2-\delta}$ and (110) plane of bcc Fe phase are clearly exhibited in the xrd pattern^{18,19,20} shown in FIG.1, whereas peak ap-

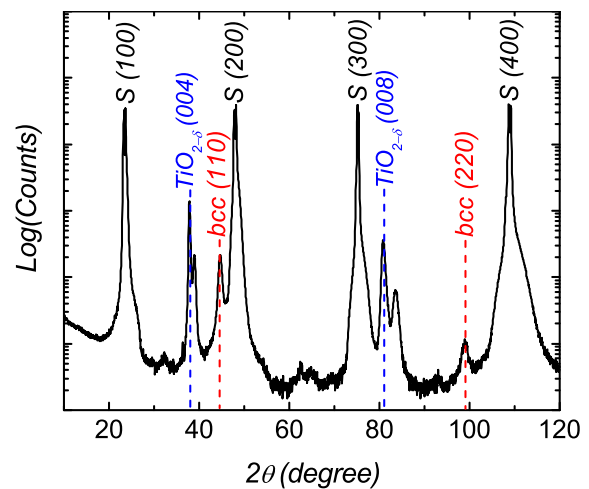


FIG. 1: X-ray diffraction pattern shows anatase of (001) $\text{TiO}_{2-\delta}$ and (110) bcc phase.

peared at $2\theta = 32.20^\circ$ could not be readily indexed. From our speculation, the peak may be originated by possible presence of iron oxide (FeO or Fe_2O_3), or ilmenite (FeTiO_3) phase.

In FIG.2, reflection electron diffraction (see upper inset) supports the existence of the epitaxial $\text{TiO}_{2-\delta}$ film host while the TEM image (and lower inset) reveal the presence of nano granular (NG) metallic Fe particles suspended within the $\text{TiO}_{2-\delta}$ host. A JOEL 2000EX high resolution transmission electron microscope operating at 200 keV and 400 keV was used in the analysis. A HRTEM image shown in FIG.2 illustrates that NG metallic Fe spheres were formed at the interface between $\text{TiO}_{2-\delta}$ layers and LaAlO_3 substrate. Average diameter of NG spheres was measured to be in the order of ≈ 10 to 15 nm as shown in the TEM image. The image suggests that the AT-PLD process may lead implantation of NG metal-

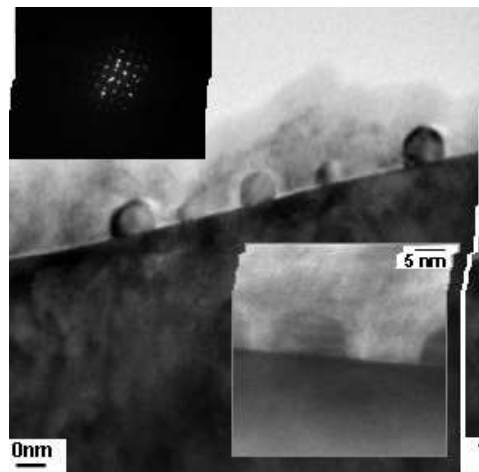


FIG. 2: TEM images for a representative film of nano granular Fe in $\text{TiO}_{2-\delta}$.

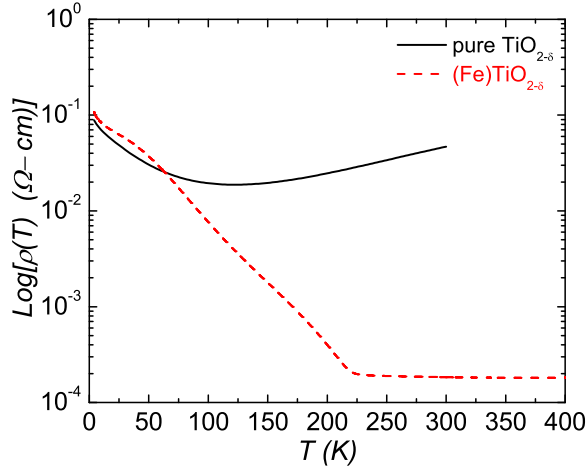


FIG. 3: Resistivity, ρ as a function of temperature, T , for the nano granular Fe in $\text{TiO}_{2-\delta}$ film (dashed line) and the pure $\text{TiO}_{2-\delta}$ (solid line) from the reference¹⁰.

lic Fe spheres into host $\text{TiO}_{2-\delta}$. Average atomic ratio of Fe/Ti ions of the AT-PLD films was obtained by energy dispersive x-ray spectroscopy (EDXS) within an ultra high resolution scanning electron microscope (UHR-SEM) column of Hitachi S-4800 that $\approx 6 \pm 0.5\%$ of Fe are possibly presented in the $1 \times 1 \text{ cm}^2$ area of the films.

For steady currents and with the magnetic intensity \mathbf{H} directed normal to the film, the resistance matrix \mathbf{R} in the plane of the film may be written as²¹

$$\mathbf{R} = \begin{pmatrix} R_{xx} & R_{xy} \\ R_{yx} & R_{yy} \end{pmatrix} = \frac{1}{t} \begin{pmatrix} \rho & -\rho_H \\ \rho_H & \rho \end{pmatrix} \quad (1)$$

wherein ρ and ρ_H represent, respectively, the normal-resistivity and the Hall resistivity. A ρ as a function of temperature for the film was measured in an applied field of $\mathbf{H} = 0 \text{ Oe}$ and shown in FIG.3. We note that the value of $\rho(T)$ was quite small at high temperature. The $\rho(T)$ behavior for pure $\text{TiO}_{2-\delta}$ film⁹ (solid line) is also shown in FIG.3 exhibiting a typical metal-insulator transition in the temperature range of 4 K and 300 K. In contrast to the ρ for pure $\text{TiO}_{2-\delta}$, ρ for the composite NG metallic Fe and $\text{TiO}_{2-\delta}$ film is a factor of 1000 lower and is constant for temperatures between 225 K and 400 K. The temperature variations are of the characteristic form expected from metal semiconductor interfaces. The ρ value at 300 K was measured to be $183 \mu\Omega\text{-cm}$, and is about a factor of 20 larger than resistivity of pure Fe²².

Presence of these unique transport properties in the NG metallic Fe spheres embedded in $\text{TiO}_{2-\delta}$ films have been modeled as coexisting electronic structures of both semiconducting $\text{TiO}_{2-\delta}$ and NG metallic Fe. We have modeled the mechanism for transport in this composite film in a sketch shown in FIG.(4)a^{17,23,24}. A common chemical potential energy or Fermi energy in both $\text{TiO}_{2-\delta}$ and metallic Fe implies that the conduction band of $\text{TiO}_{2-\delta}$ is degenerate with the metallic Fe conduction

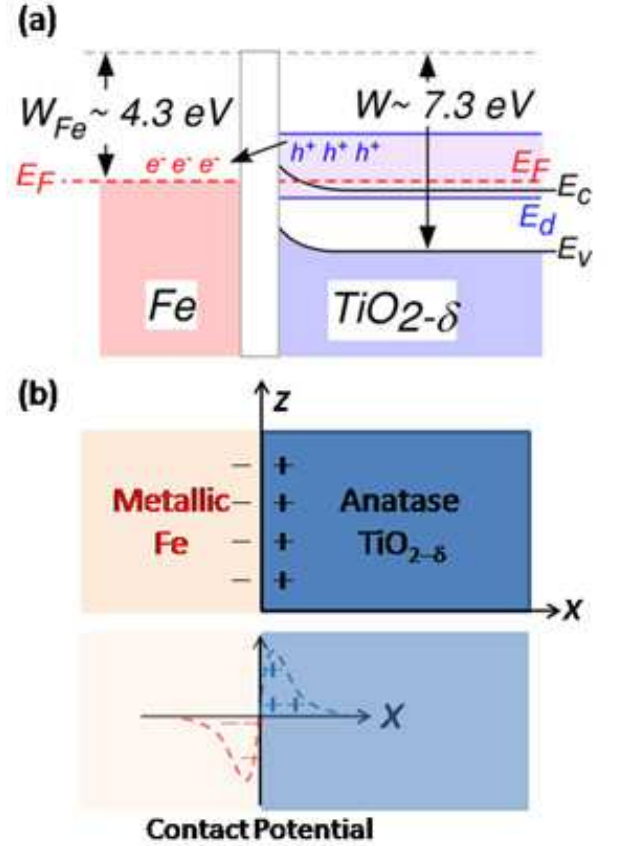


FIG. 4: (a) Energy band structure of nano granular metallic Fe and semiconducting $\text{TiO}_{2-\delta}$, where it is similar to metal oxide semiconductor. (b) Contact potential model.

band. Since the Fermi energy in metallic Fe is about 4.6 eV above the conduction energy level it implies that the energy band gap (3 eV) of $\text{TiO}_{2-\delta}$ is degenerate with the iron conduction band. This means that the donor levels in $\text{TiO}_{2-\delta}$ are also degenerate, and thereby, electrons hopping between Ti^{2+} and Ti^{3+} sites would find a conduit into the metallic conduction band leaving behind holes in $\text{TiO}_{2-\delta}$. Therefore, a small potential barrier must exist at the interface. This is illustrated schematically in FIG.4a. As noted in FIG.2, the NG metallic Fe sphere particles are isolated or disconnected, implying that conduction in the $\text{TiO}_{2-\delta}$ is via hole conduction. This can be also explained by contact potential at the interface between NG metallic Fe sphere and anatase $\text{TiO}_{2-\delta}$ as described in Landau Lifshitz²¹. In order to remove electron trough the surface of a metallic Fe, work must be done thermodynamically. According to the reference²¹, Poisson's equation for potential $\Phi(x)$ along the x -axis normal to the interface between NG metallic Fe / $\text{TiO}_{2-\delta}$ implies

$$\begin{aligned} -\Phi''(x) &= 4\pi\rho(x), \\ \varpi &= \int_{-\infty}^{\infty} x\rho(x)dx = -\frac{1}{4\pi} \int_{-\infty}^{\infty} x\Phi''(x)dx, \\ \Phi(\infty) - \Phi(-\infty) &= V_c = 4\pi\varpi, \end{aligned} \quad (2)$$

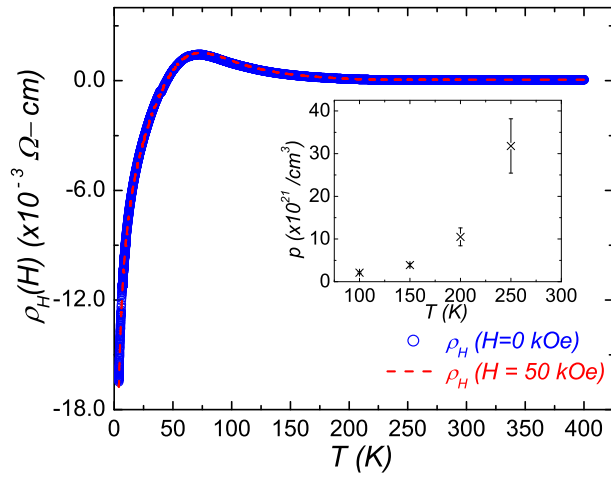


FIG. 5: (Hall resistivity, $\rho_H(H)$, versus temperature for $H = 0$ (circle symbol) and $H = 50.0$ kOe (dashed line) in the nano granular Fe in $\text{TiO}_{2-\delta}$ film. Inset shows relation carrier density in function of temperature..

wherein ϖ is defined to be dipole moment per unit contact area and V_c is contact potential. The schematic of contact potential at the interface is shown in FIG.4b.

Electron conduction between metallic spheres may not be possible, see FIG.2. In FIG.5, Hall resistivity is plotted as a function of temperature that at high temperatures carriers are holes which also confirmed by Seebeck measurements. Furthermore, the number of carriers relative to pure $\text{TiO}_{2-\delta}$ has increased by factor 1,000 and the mass of holes is approximately about 10 times larger than the electron mass¹⁰. Also, in FIG.5 the carrier hole density p is plotted as a function of temperature. In order to calculate p , we employ

$$\rho_H = R_0 B + 4\pi M R_S \quad \text{and} \quad R_0 = \frac{1}{pec}, \quad (3)$$

wherein R_0 and R_S are the normal and anomalous Hall coefficients, respectively. In FIG.6, $\rho_H(H)$ scales linearly with magnetic field for temperatures below 300 K. The slope of $\rho_H(H)$ vs. H gives rise to the normal Hall coefficient which corresponds to the first term in Eq.(3), where the hole carrier density, p , may be deduced. For temperatures well above 250 K, p is governed by the second term in Eq.(3), the anomalous Hall coefficient. Eq.(3) may re-written as²⁵

$$\rho_H = \frac{H}{pec} + \left(\frac{1}{pec} + R_S \right) (4\pi M) \quad \text{where} \quad R_S \gg R_0. \quad (4)$$

The anomalous Hall effect is dominant at high temperatures ($T > 250$ K) and the second term in Eq.(4) is constant for saturation magnetization $M = M_S$.

The spontaneous magnetization, $M(H, T)$, was measured to be nearly constant as a function of temperature as shown in FIG.7. The measurement was performed with an external dc-magnetic field of 10.0 kOe applied

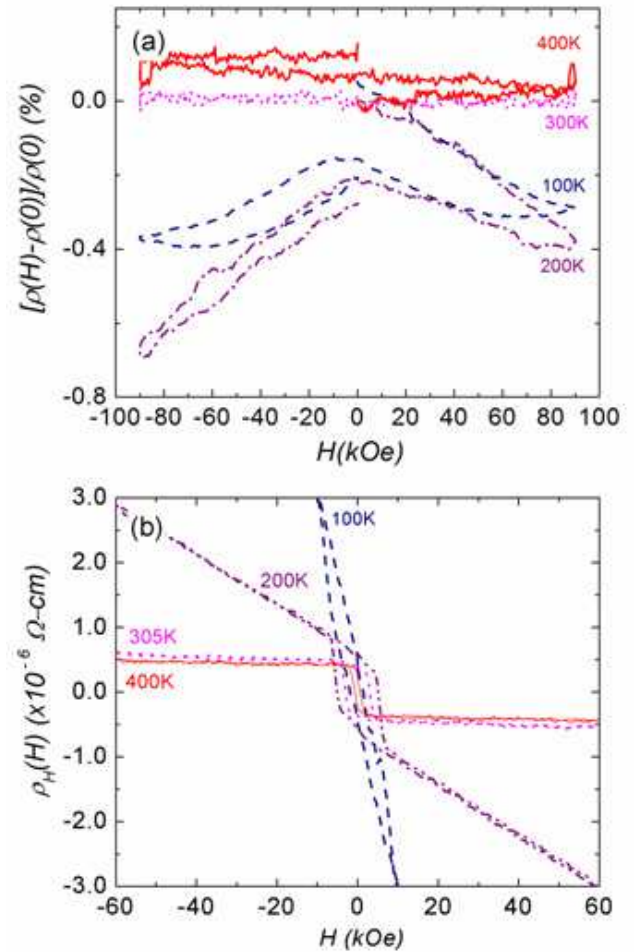


FIG. 6: (a) Magneto resistivity, $\rho(H)$ versus H in different temperatures. (b) Hall resistivity, $\rho_H(H)$ versus H in different temperatures.

normal to the film plane (out-of-plane measurement). The film can be fully saturated with a field of ≈ 6.6 kOe, since the coercive field was measured to be 2.0 kOe. Field cooled (FC) and zero-field-cooled (ZFC) $M(H, T)$ data in FIG.7 shows no difference which implies that no spin glass effects are present in the films. There are two sources for magnetism in this composite structure: (1) ferromagnetism in $\text{TiO}_{2-\delta}$ and (2) ferromagnetism in metallic Fe spheres. The ferromagnetism in $\text{TiO}_{2-\delta}$ is due to double exchange as calculated by us in a previous calculation and it gives rise to a relatively small saturation magnetization at room temperature (≈ 400 Gauss). Based on the data presented in FIG.2, we estimate a sphere density of 0.125 to 0.25×10^{18} spheres/ cm^3 and sphere diameter between 10 and 15 nm. This implies that the loading factor of metallic Fe in the composite film is in the order of 0.05 to 0.25 which corresponds

to 1,100 to 5,100 Gauss for the saturation magnetization of the composite. This compares with a measured value of 3,100 Gauss. We have measured the transverse magnetoresistivity, $\rho(H)$, and Hall resistiv-

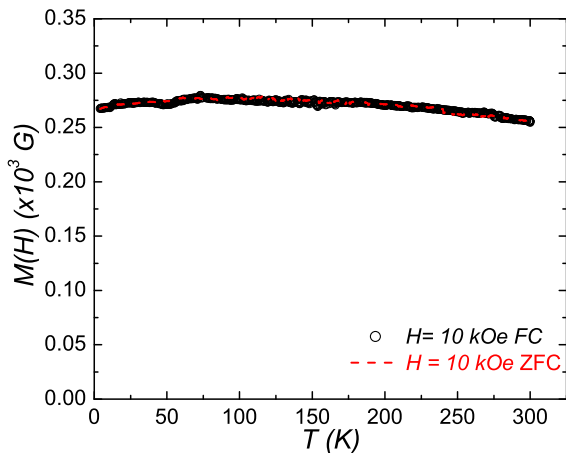


FIG. 7: Static magnetization, $M(H, T)$, versus temperature with $H = 10.0$ kOe normal to the film plane.

ity, $\rho_H(H)$, as a function of magnetic field sweeps between -90 and $+90$ kOe as shown in FIGS.6a and 6b, and at different temperatures. In FIG.6a, the normal resistivity exhibits negative magnetoresistivity defined as, $\Delta f = (\rho(H) - \rho(0))/\rho(0)$ for temperatures $100 K < T < 200 K$. Δf is negligible for temperatures above $300 K$. However, plots of $\rho_H(H)$ shown in FIG.6b, clearly demonstrate that saturation effects at temperatures near room temperature as a result of the hole carrier density increasing toward saturation levels, see FIG.3. Notice that plots of $\rho_H(H)$ at $T \geq 200 K$ exhibit clear hysteresis loop behavior similar to ferromagnetic hysteresis loops. Interestingly, saturation for both $\rho_H(H)$ and (M/M_S) , normalized magnetization, occurred at exactly the same external magnetic field value of ≈ 6.6 kOe, see FIG.8. This is no coincidence, since one requires a demagnetization factor of $(4\pi/3)$ to magnetically saturate a sample of spherical shape in order to overcome a

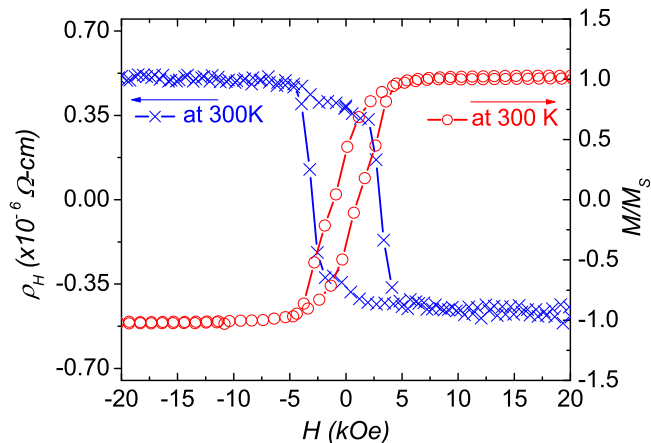


FIG. 8: Symbol (X) shows a typical anomalous Hall hysteresis loop, $\rho_H(H)$, at $T = 300$ K with magnetic hysteresis loop (symbol (o)) at 300 K.

magnetic field of 6.8 kOe in Fe spheres at (say) room temperature. These data also show relatively smaller coercive field for the (M/M_S) hysteresis loop than for the $\rho_H(H)$ hysteresis loop. The difference in hysteresis loops is due to the fact that the NG Fe spherical samples give rise to dipole internal magnetic fields. In order to reverse the magnetization in each sphere it requires an external field to overcome this interactive internal field. Hence, the coercive field is approximately constant with temperature as it scales with magnetization. In the Hall resistivity measurement the coercive field is strongly temperature dependent, since there are two contributions to the resistivity measurement: (1) Normal Hall resistivity contribution which is not hysteretic with respect to \mathbf{H} and (2) the anomalous Hall effects which is hysteretic with \mathbf{H} , since this effect is proportional to the magnetization. At high temperatures the AHE contribution dominates the resistivity measurement in contrast to low temperatures where the normal Hall contribution dominates. Thus, spin polarization as reflected in $\rho_H(H)$, see FIG.8, correlates extremely well with the magnetic hysteresis loop implying that the magnetized Fe spheres are polarizing the carriers.

III. DISCUSSION AND CONCLUSIONS

The plots of $\rho_H(H)$ at $T < 200 K$ exhibit paramagnetic hysteresis behavior, see FIG.6b. This transition between paramagnetic and ferromagnetic $\rho_H(H)$ hysteresis behavior was also reported and correlated with hole carrier density related with RKKY theory in previous research^{1,26}. Their estimate of the threshold hole density for the carrier spin polarization transition was $p = 3 \times 10^{20}/\text{cm}^3$ from paramagnetic $p < 3 \times 10^{20}/\text{cm}^3$ to ferromagnetic $p \geq 3 \times 10^{20}/\text{cm}^3$ behavior^{1,25,26}. Our estimate of hole carrier density of the films was $p \approx 2.1 \times 10^{21}/\text{cm}^3$ and $p \approx \times 10^{22}/\text{cm}^3$ at $T = 100 K$ and $200 K$, respectively. The film exhibited strong polarization and hysteresis behavior as a function of applied field at $300 K$. Since anomalous Hall effects may be observed in the presence of spontaneous magnetization^{27,28}, we infer that about $\approx 10^{22}/\text{cm}^3$ hole carriers are polarized by an applied field \mathbf{H} . This indicates that nearly all of the carriers were polarized by the spontaneous magnetization at $T = 300 K$. According to FIG.8, carrier polarization correlated very well with the magnetic hysteresis loop of NG Fe spheres. Also, FIG.8 indicates that the carrier polarization is not affected by external fields up to 3.0 kOe, which can be an advantage for memory device applications^{29,30}. However, if the shape of the particles embedded in the composite could be shaped into needles, it would imply spin polarization of carriers in external magnetic fields below 0.1 kOe which is ideally suited for spintronics applications.

In summary, magnetic and magneto-transport data for films of nano granular metallic Fe and oxygen defected $\text{TiO}_{2-\delta}$ are reported. The essence of this paper showed

that conduction carriers of the films were strongly coupled to residual magnetic moments of metallic Fe grains in the nano composite structure. The dramatic reduction of normal resistivity ($\rho(T)$) of the films is a consequence of two factors: (1) oxygen defects in the $\text{TiO}_{2-\delta}$ host induced electron hopping; (2) electrons from the $\text{TiO}_{2-\delta}$ were introduced into the conduction band of Fe to create holes in $\text{TiO}_{2-\delta}$ similar to a Metal Oxide Semiconductor (MOS) structure. As a result the number of carriers increased at room temperature. The holes in $\text{TiO}_{2-\delta}$ were polarized due to the presence of ferromagnetic nano granular metallic Fe, where the carrier polarized density

was measured to be near $\geq 3.0 \times 10^{22} / \text{cm}^3$. Therefore, spintronics and spin dependent memory applications can be based upon the results presented here.

IV. ACKNOWLEDGMENT

This research was supported by the National Science Foundation (DMR 0400676) and the Office of Naval Research (N00014-07-1-0701).

-
- * Corresponding author e-mail: syoon@ece.neu.edu
 † Electronic address: vittoria@lepton.neu.edu
 ‡ Electronic address: harris@ece.neu.edu
 § Electronic address: allan.widom@gmail.com
- ¹ H. Ohno, *Science* **281**, 951 (1998).
 - ² K. Ueda, H. Tahata, and T. Kawai, *Appl. Phys. Lett.* **79**, 988 (2001).
 - ³ Y. Masumoto *et al.*, *Science* **291**, 854 (2001).
 - ⁴ S.J. Pearton *et al.*, *Mat. Sci. and Engn.* **R40**, 137 (2003).
 - ⁵ S.A. Chambers and R.F.C. Farrow, *MRS Bulletin* **28**, 729 (2003).
 - ⁶ I. Žutić, J. Fabian, and D. Sarma, *Rev. Mod. Phys.* **76**, 32 (2004).
 - ⁷ J.M.D. Coey, M. Venkatesan, and C.B. Fitzgerald, *Nat. Mater.* **4**, 173 (2005).
 - ⁸ N. H. Hong *et al.*, *Phys. Rev.*, **B 73**, 132404 (2006).
 - ⁹ S.D. Yoon *et al.*, *J. Phys.: Condens. Matter.* **18**, L355 (2006).
 - ¹⁰ S.D. Yoon *et al.*, *J. Phys.: Condens. Matter.* **19**, 326202 (2007).
 - ¹¹ M. Earle, *Phys. Rev.* **61**, 56 (1942).
 - ¹² R.G. Breckenridge and W.R. Hosler, *Phys. Rev.* **91**, 793 (1953).
 - ¹³ N. Daude, C. Gout, and C. Jouanin, *Phys. Rev.* **B 15**, 3229 (1977).
 - ¹⁴ J. Pascual, J. Camassel, and H. Mathieu, *Phys. Rev.* **B 18**, 5606 (1978).
 - ¹⁵ H. Tang *et al.*, *Solid State Commun.* **87**, 847 (1993).
 - ¹⁶ S.A. Campbell *et al.*, *IBM J. Res. Develop.* **43**, 383 (1999).
 - ¹⁷ B.G. Streetman, “*Solid State Electronic Devices*,” ch. 8, 301, Prentice Hall, Inc., Englewood Cliffs, New Jersey (1990).
 - ¹⁸ *Natl. Bur. Stand. (U.S.) Monogr.* 25 **7**, 82 (1969).
 - ¹⁹ C.J. Howard, T.M. Sabine, and F. Dickson, *Acta Crystallographica, B: Structural Science* **B47**, 462 (1991).
 - ²⁰ H.E. Swanson, J.C. Doukhan, and G.M. Ugrinic, *Natl. Bur. Stand. (U.S.), Circ.* **5**, 539 (1955).
 - ²¹ L.D. Landau and E.M. Lifshitz, “*Electrodynamics of continuous media*,” 1984 ch. 4, Pergamon Press, Oxford (1984).
 - ²² R.C. Weast and M.J. Astle, “*CRC Handbook of chemistry and physics*,” section E, 81, CRC press, Inc. Boca Raton, Florida, 63rd edition (1982).
 - ²³ M.L. Knotek and P.J. Feibelman, *Phys. Rev. Lett.* **40**, 964 (1978).
 - ²⁴ Z. Zhang, S.P. Jeng, and V. Henrich, *Phys. Rev.* **B 43**, 12004 (1991).
 - ²⁵ C. M. Hurd, “*The Hall Effect in Metals and Alloys*,” 1972 Ch. 5, Plenum Press, New York London.
 - ²⁶ T. Story, *et al.*, *Phys. Rev. Lett.* **56**, 777 (1986).
 - ²⁷ C.L. Chien and C.R. Westgate, “*The Hall effect and its applications*,” Plenum Press, New York and London (1980).
 - ²⁸ R. Karplus and J. M. Luttinger, *Phys. Rev.* **95**, 1154 (1954).
 - ²⁹ G. Prinz, *Science* **282**, 1660 (1998).
 - ³⁰ S.A. Wolf *et al.*, *Science* **294**, 1488 (2001).